JACS
JOURNAL OF THE AMERICAN CHEMICAL SOCIETY
Communication
pubs.acs.org/JACS

Flexible Solid-State Supercapacitor Based on a Metal–Organic Framework Interwoven by Electrochemically-Deposited PANI

Lu Wang,[†,§] Xiao Feng,[†,§] Lantian Ren,[†] Qiuhan Piao,[†] Jieqiang Zhong,[†] Yuanbo Wang,[‡] Haiwei Li,[†] Yifa Chen,[†] and Bo Wang*[,†]

[†]Key Laboratory of Cluster Science, Ministry of Education of China, School of Chemistry, Beijing Institute of Technology, 5 South Zhongguancun Street, Beijing 100081, P. R. China

[‡]School of Chemical Engineering and Technology, Tianjin University, 92 Weijin Avenue, Tianjin 300072, P. R. China

Supporting Information

ABSTRACT: Metal–organic frameworks (MOFs) have received increasing attention as promising electrode materials in supercapacitors (SCs). Yet poor conductivity in most MOFs largely thwarts their capacitance and/or rate performance. In this work, an effective strategy was developed to reduce the bulk electric resistance of MOFs by interweaving MOF crystals with polyaniline (PANI) chains that are electrochemically deposited on MOFs. Specifically we synthesized cobalt-based MOF crystals (ZIF-67) onto carbon cloth (CC) and further electrically deposited PANI to give a flexible conductive porous electrode (noted as PANI-ZIF-67-CC) without altering the underlying structure of the MOF. Electrochemical studies showed that the PANI-ZIF-67-CC exhibits an extraordinary areal capacitance of 2146 mF cm^{-2} at 10 mV s^{-1}. A symmetric flexible solid-state supercapacitor was also assembled and tested. This strategy may shed light on designing new MOF-based supercapacitors and other electrochemical devices.

The development of flexible, low-cost, and high performance energy storage system is crucial to meet the growing needs for portable electronic devices such as foldable phones and wearable electronics. Supercapacitors (SCs) with high power density and long cycle life have drawn great attentions by virtue of their balanced rate performance and energy density.[1] Among these SCs, flexible solid-state supercapacitors (SSCs) are considered to be promising candidates for electrochemical energy storage toward lightweight, safe, eco-friendly, and easy-to-handle devices since they avoid using liquid electrolyte and can be easily folded or attached to any surfaces.[2] To achieve high electrochemical performance, high conductivity and large electrolyte-accessible surface areas are, among others, two major prerequisites for the active materials used in the SCs.[3] Emerging as a new class of porous materials with exceptional porosities and well-defined pores, metal–organic frameworks (MOFs) are constructed by joining metal ions with organic links. In addition to the huge progress in expanding new MOF families and exploiting their applications including gas storage and separation,[4] catalysis,[5] sensor,[6] and drug delivery,[7] quite recently, several pioneering work have also been done on energy storage systems using MOFs.[8]

Up to date, various MOF-based SCs have been developed, and generally these SCs can be classified into three types, SCs that are fabricated by (i) utilizing pristine MOFs to store electrical energy on their internal surfaces through electrochemical double-layer capacitor (EDLC) mechanism or exploiting the redox reaction of metal center to store energy;[9] (ii) destroying MOFs to afford metal or metal-oxides and storing energy Faradaically via the charge transfer between the electrolyte and electrode;[10] (iii) pyrolyzing MOFs to give microporous carbons and enhancing the capacitance through increasing the conductivity.[11] However, these approaches either give relatively low capacitance or show a limited cycling ability, which hindered them from being used as a general method to prepare MOF-based SCCs.

Metal–organic frameworks are well-known for their high surface areas. Thus, ions in the electrolytes are allowed to access the micropores and/or mesopores in MOFs by diffusion effect. Electrolytes can easily get inside the pores and pass out, which endows MOFs with great opportunities to generate large EDLC capacitance. Unfortunately, MOFs are mostly nonconductive (Scheme 1a), and as a result, it is challenging to build effective SCs based on pure MOFs.

Inspired by the pioneering work by Yaghi et al. using MOF crystals for SCs with high areal capacitance,[12] herein, we report a

Scheme 1. Schematic Representation of Electron and Electrolyte Conduction in (a) MOF and (b) MOF Interwoven by PANI[a]

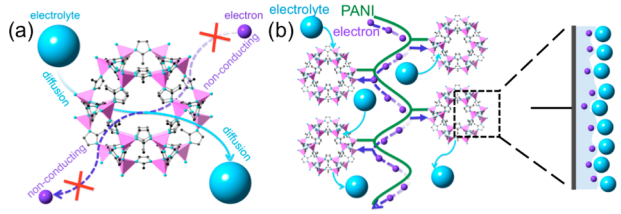

[a](a) Electron cannot migrate along or access the skeleton of MOF crystals, while electrolyte can get in and out of the MOF pores by diffusion effect. (b) After interweaving MOF crystals with conductive PANI, both electron and electrolyte can access MOF surfaces and an electrochemical double-layer is formed on the surface of PANI-ZIF-67-CC.

Received: February 12, 2015
Published: April 11, 2015

DOI: 10.1021/jacs.5b01613
J. Am. Chem. Soc. 2015, 137, 4920–4923

new strategy for achieving high performance SCs and overcoming the insulating problems of MOFs by electrochemically interweaving MOF crystals with a conductive polymer, polyaniline (PANI) (Scheme 1b). After electrochemical deposition, the isolated MOF crystals are interconnected and linked up by the chains of PANI that act as bridges for electrons transportation between the external circuit and the internal surface of MOFs. A synergistic effect is observed in this approach. The deposited PANI can efficiently improve the conductivity of MOFs and enhance Faradaic processes across the interface. Therefore, such hybrid-structured electrode takes the advantages of both high EDLC capacitance originated from the internal surface areas of MOFs and effective pseudocapcitance generated by PANI.

Specifically we selected ZIF-67, a Co-based MOF, as the electrical charge storing material. Carbon cloth, which is an cost-effective and highly conductive textile with outstanding mechanical flexibility and strength,[2d] was used as both substrate and current collector to achieve flexibility. ZIF-67 was first deposited on the carbon cloth and then electrochemically linked by PANI, and thus-obtained electrode is denoted as PANI-ZIF-67-CC. An exceptional areal capacitance of 2146 mF cm^{-2} at 10 mV s^{-1} for PANI-ZIF-67-CC in a three-electrode system was achieved. Moreover, a flexible SSC device was constructed based on two symmetric freestanding PANI-ZIF-67-CC electrodes. The SCC yielded a remarkable areal capacitance of 35 mF cm^{-2} and a power density of 0.833 W cm^{-3} at a current density of 0.05 mA cm^{-2} and retained more than 80% of its initial capacitance after 2000 cycles.

The two-step fabrication process of PANI-ZIF-67-CC electrode is illustrated in Figure 1. First, a slurry of 70 wt % active material (ZIF-67) with 20 wt % conductive Super P and 10 wt % poly(vinylidene fluoride) (PVDF) binder in NMP was casted on carbon cloth. The afforded ZIF-67/carbon cloth electrode (denoted as ZIF-67-CC) still maintains the excellent mechanical strength and flexibility. Scanning electron microscopy (SEM) reveals that ZIF-67 crystals with sizes around 300 nm are anchored and well distributed across the surface of each carbon cloth fiber (Figures 1c,d and S1). Second, ZIF-67-CC was interconnected by conductive PANI by electropolymerization from the monomer aniline under the cycling potential. The cyclic voltammograms of the electropolymerization process of aniline is shown in Figure S2. Thus-obtained PANI-ZIF-67-CC was washed and dried at 80 °C. Typically, about 7.0 mg of ZIF-67 and 1.0 mg of PANI was coated on the 1 × 2 cm^2 carbon cloth. The SEM image shows that a remarkable morphology change takes place on the external surface of ZIF-67 crystals after electropolymerization of aniline (Figures 1e,f and S3). PANI chains are not only coated on the surface of MOFs but also interconnected isolated MOF crystals and act as bridges between the MOF particles. Conductive PANI covers the interparticle open space and links up the crystals of ZIF-67.

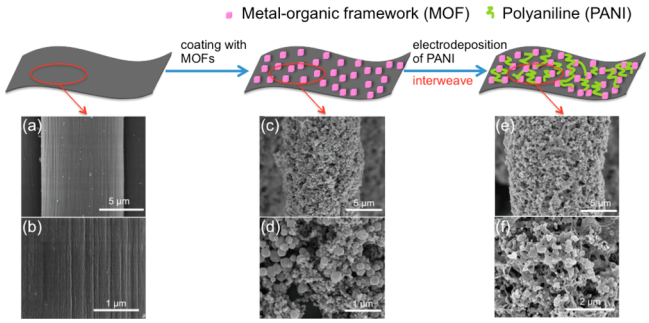

Figure 1. Schematic illustration of the two-step fabrication process of PANI-ZIF-67-CC electrode and SEM images of (a,b) the carbon cloth fibers, (c,d) after coating with ZIF-67, and (e,f) after electropolymerization of aniline.

The powder X-ray diffraction (PXRD) patterns of ZIF-67-CC and PANI-ZIF-67-CC are consistent with that of the pristine ZIF-67, demonstrating that they maintain crystallinities and underlying topologies after coating and electropolymerization (Figure S4). Nitrogen adsorption measurements at 77 K were conducted to investigate the pore structures of the samples. The BET surface areas of ZIF-67, ZIF-67-CC, and PANI-ZIF-CC are calculated to be 1717, 450, and 73 m^2 g^{-1}, respectively, which indicates the porous nature of PANI-ZIF-67-CC even after electropolymerization (Figures S5 and S6). The pore size distributions evaluated by nonlocal density functional theory method indicates that the amount of the micropores in ZIF-67 are significantly decreased and that the pore volume originated from the space between the MOF particles is also diminished. The decrement of surface area and pore size indicate that the PANI not only covers the interparticle open space between the particles but also penetrates into some of the internal micropores, which allows the electron to access to the internal surface of ZIF-67. It should be noted that although the pores in ZIF-67 are partially blocked by PANI, the electrolyte can also enter the pores via diffusion[13] confirmed by further electrical performance evaluation.

We further characterized the chemical nature of the PANI formed in PANI-ZIF-67-CC by X-ray photoelectron spectroscopy (XPS) since the conductivity of PANI is dependent on the ratio of the protonated emeraldine salt in it. The deconvolution of N 1s core-level spectra resulted in three peaks (Figure S7a): the quinonoid imine centered at 397.6 eV, the benzenoid amine at 398.7 eV, and the positively charged nitrogen at 404.5 eV.[14] Accordingly, the ratio of ═N− and −NH− components provides a direct measurement of the intrinsic oxidation state of PANI, and the N^+/N ratios indicate the proton doping level of the polymer.[15] Based on the quantitative analysis of the deconvoluted N (1s) spectra of PANI-ZIF-67, the ═N−/−NH− and N^+/N ratios are 0.76 and 0.1, respectively. Considering that ZIF-67 contributes to the peaks at 397.6 and 398.7 eV due to the existence of quinonoid imine and benzenoid amine (Figure S7), we can conclude that the N^+/N ratio of PANI in PANI-ZIF-67 composite is much higher than 0.1, and thus, the PANI can provide an efficient pathway for electron conduction. The Nyquist plots of ZIF-67-CC and PANI-ZIF-67-CC (Figure 2a) were analyzed by applying the equivalent circuit shown in Figure S8. The best-fit calculation showed that the equivalent internal resistance (R_s) is decreased from 4.428 to 3.582 Ω. After PANI deposition, ions can easily accumulate on the surface of the electrode. The hydrophilic property of PANI makes the surface of the electrode, which used to be hydrophobic, much easier to get wetted. Therefore, the electrolyte ions obtain access to the inner pores of PANI-ZIF-67. As a result of electrical double layer capacitance, the capacitance would be improved.[16] The straight line of PANI-ZIF-67-CC at low frequency, which is nearly paralleled to the imaginary axis, indicates typical EDLC behavior.

The electrochemical performance of PANI-ZIF-67-CC electrode was studied in a three-electrode cell using 3 M KCl as electrolyte. Based on the cyclic voltammetry (CV) curves of PANI-ZIF-67-CC electrode at 10 mV s^{-1} (Figure 2b), the specific capacitance of PANI-ZIF-67-CC is 371 F g^{-1} according to the mass of activated material. Although only the specific

DOI: 10.1021/jacs.5b01613
J. Am. Chem. Soc. 2015, 137, 4920−4923

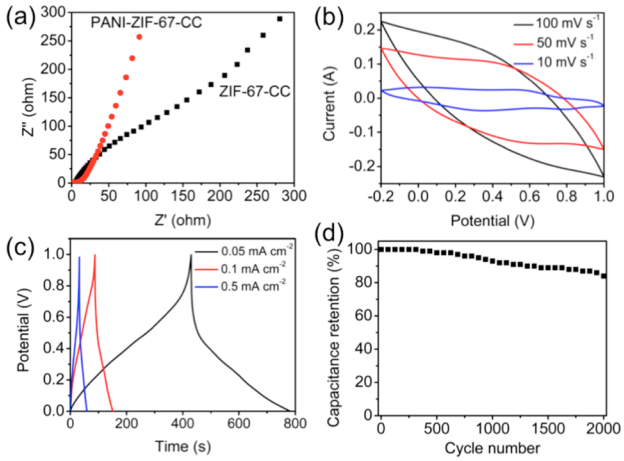

Figure 2. (a) Nyquist electrochemical impedance spectra of ZIF-67-CC and PANI-ZIF-67-CC. (b) Cyclic voltammograms collected of PANI-ZIF-67-CC electrode at different scan rate in 3 M KCl. (c) Galvanostatic charge/discharge curves of the solid-state SC device at different current densities. (d) Cycling performance of the solid-state SC device measured at 0.1 mA cm^{-2} for 2000 cycles.

capacitance of PANI-CC itself can reach 469 F g^{-1} through faradic process, majority of the capacitance for PANI-ZIF-67-CC is derived from ZIF-67 through EDLC process due to the fact that the mass ratio of PANI/ZIF-67 in PANI-ZIF-67-CC is 1 to 7.

Areal capacitance is very important to reflect the effective specific capacitance of the electrode in applications such as flexible and wearable electronics. Maximum areal capacitances of 2146, 1466, and 901 mF cm^{-2} for PANI-ZIF-67-CC electrode were obtained at the scan rates of 10, 50, and 100 mV s^{-1}, respectively (Figure S9d). In contrast, ZIF-67-CC showed an areal capacitance of 1.47 mF cm^{-2} at 10 mV s^{-1} (Figure S9b), resulting from its insulating nature. It is worth noting that although PANI-CC can reach high gravimetric capacitance, its areal capacitance is only 727 mF cm^{-2} at the same scan rate (Figure S9c), which is only one-third of that of PANI-ZIF-67-CC (Figure 3). These results demonstrate that a synergistic effect occurs upon interweaving ZIF-67 aggregates with PANI, the hybrid-structured electrode benefits from both EDLC capacitance of the internal surface areas of MOFs and the pseudocapcitance of PANI. The value of 2146 mF cm^{-2} for areal capacitance of PANI-ZIF-67-CC electrode is the highest among all MOF-based SCs reported to date and surpasses the

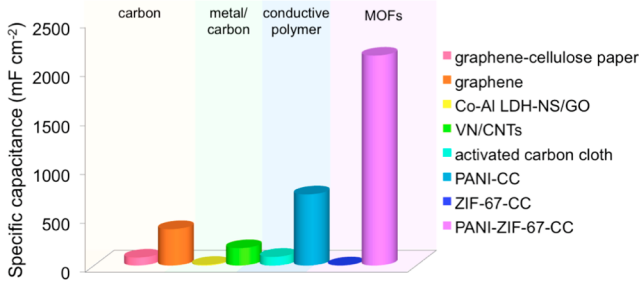

Figure 3. Areal capacitances of the literature reported supercapacitors and that of PANI-ZIF-67-CC presented in this Communication. The PANI-CC and ZIF-67-CC are control experiments. Co–Al LDH-NS/GO: Co–Al layered double hydroxide nanosheets (Co–Al LDH-NS) and graphene oxide (GO). VN/CNTs: VN/carbon nanotubes.

values of most SCs electrode materials, such as carbon nanoparticles (CNPs), carbon nanotubes (CNTs), graphene, conductive polymers, and metal oxides (Table S1).[3,17]

Further, we fabricated a flexible symmetric all-solid-state super capacitor device. Two identical pieces of PANI-ZIF-67-CC electrode with an area of 1 × 2 cm^2 were placed in parallel and H_2SO_4/poly(vinyl alcohol) was used as the gel electrolyte (Figure 4a). Based on the galvanostatic charge/discharge curves

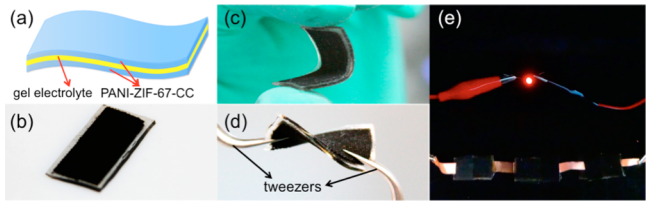

Figure 4. (a) Schematic illustration of PANI-ZIF-67-CC flexible solid-state SC device. (b–d) Optical photographs of the fabricated flexible solid-state SC device under (b) normal, (c) bent, and (d) twisted state. (e) Photograph of a red light-emitting-diode (LED) powered by the three SCs connected in series.

of thus-obtained solid-state SCs at the scan rate of 0.05 mA cm^{-2} (Figure 2c), the areal capacitance of the device is calculated to be 35 mF cm^{-2}, while the stack capacitance is 116 mF cm^{-3}. The highest power density of 0.833 W cm^{-3} (0.245 W cm^{-2}) and the maximum energy density of 0.0161 mWh cm^{-3} (0.0044 mWh cm^{-2}) were achieved. As shown in Figure 2d, the all-solid-state supercapacitor retains more than 80% of its initial capacitance after 2000 cycles at 0.1 mA cm^{-2}. The stability of ZIF-67 after charging–discharging is proved by PXRD (Figure S4).

We also tested the performance of such device in various practical conditions, in which a piece of gel electrolyte serving as a separator was sandwiched by two identical pieces of PANI-ZIF-67-CC electrodes (Figure 4a). The electrical performance of the device did not deteriorate even after bending and twisting (Figure 4b–d). We evaluated the capability of using these SSC devices to power small electronic devices, such as a light-emitting-diode (LED). Three SSCs were connected in series and charged by two 14500 batteries in series for 30 s, and a red LED was successfully lighted up by these SCs (Figure 4e). These suggest the potential of such MOF-based solid-state SCs for flexible and wearable electronics.

In summary, we demonstrated a strategy to design and fabricate a flexible MOF-based SC, by interweaving ZIF-67 crystals that are coated on carbon cloth with electrochemically polymerized PANI. An unprecedented high areal capacitance of 2146 mF cm^{-2} at 10 mV s^{-1} was achieved. This value is the highest among all MOF-based SCs reported to date and surpasses those of most SCs that are based on CNPs, CNTs, graphene, conductive polymers, and metal oxides. Moreover, a flexible solid-state SC based on MOFs was fabricated for the first time. This may pave the way for developing novel flexible solid-state SCs with exceptional electrochemical performance and potential applications as portable energy storage devices and wearable electronics.

■ ASSOCIATED CONTENT

Ⓢ Supporting Information

Experimental details and additional characterizations. This material is available free of charge via the Internet at http://pubs.acs.org.

DOI: 10.1021/jacs.5b01613
J. Am. Chem. Soc. 2015, 137, 4920–4923

AUTHOR INFORMATION

Corresponding Author

*bowang@bit.edu.cn

Author Contributions

[§]These authors contributed equally to this work.

Notes

The authors declare no competing financial interest.

ACKNOWLEDGMENTS

This work was financially supported by the 973 Program 2013CB834704; Provincial Key Project of China (7131253); the National Natural Science Foundation of China (21471018, 21404010, and 21201018); 1000 Plan (Youth).

REFERENCES

(1) (a) Frackowiak, E.; Beguin, F. *Carbon* **2001**, *39*, 937. (b) Simon, P.; Gogotsi, Y. *Nat. Mater.* **2008**, *7*, 845. (c) Zhai, Y.; Dou, Y.; Zhao, D.; Fulvio, P. F.; Mayes, R. T.; Dai, S. *Adv. Mater.* **2011**, *23*, 4828. (d) Nishihara, H.; Kyotani, T. *Adv. Mater.* **2012**, *24*, 4473. (e) Wang, J.; Xin, H. L.; Wang, D. *Part. Part. Syst. Char.* **2014**, *31*, 515. (f) Beguin, F.; Presser, V.; Balducci, A.; Frackowiak, E. *Adv. Mater.* **2014**, *26*, 2219. (g) Zhou, G.; Li, F.; Cheng, H.-M. *Energy Environ. Sci.* **2014**, *7*, 1307.

(2) (a) Nyholm, L.; Nystrom, G.; Mihranyan, A.; Stromme, M. *Adv. Mater.* **2011**, *23*, 3751. (b) Fu, Y.; Wu, H.; Ye, S.; Cai, X.; Yu, X.; Hou, S.; Kafafy, H.; Zou, D. *Energy Environ. Sci.* **2013**, *6*, 805. (c) Dubal, D. P.; Kim, J. G.; Kim, Y.; Holze, R.; Lokhande, C. D.; Kim, W. B. *Energy Technol.* **2014**, *2*, 325. (d) Lu, X.; Yu, M.; Wang, G.; Tong, Y.; Li, Y. *Energy Environ. Sci.* **2014**, *7*, 2160. (e) Hu, L.; Cui, Y. *Energy Environ. Sci.* **2012**, *5*, 6423.

(3) Wang, G.; Wang, H.; Lu, X.; Ling, Y.; Yu, M.; Zhai, T.; Tong, Y.; Li, Y. *Adv. Mater.* **2014**, *26*, 2676.

(4) (a) Li, J.-R.; Kuppler, R. J.; Zhou, H.-C. *Chem. Soc. Rev.* **2009**, *38*, 1477. (b) Furukawa, H.; Cordova, K. E.; O'Keeffe, M.; Yaghi, O. M. *Science* **2013**, *341*, 1230444. (c) Murray, L. J.; Dinca, M.; Long, J. R. *Chem. Soc. Rev.* **2009**, *38*, 1294. (d) Dinca, M.; Long, J. R. *Angew. Chem., Int. Ed.* **2008**, *47*, 6766. (e) Sculley, J.; Yuan, D.; Zhou, H.-C. *Energy Environ. Sci.* **2011**, *4*, 2721. (f) Banerjee, R.; Furukawa, H.; Britt, D.; Knobler, C.; O'Keeffe, M.; Yaghi, O. M. *J. Am. Chem. Soc.* **2009**, *131*, 3875. (g) Eddaoudi, M.; Kim, J.; Rosi, N.; Vodak, D.; Wachter, J.; O'Keeffe, M.; Yaghi, O. M. *Science* **2002**, *295*, 469.

(5) (a) Lee, J.; Farha, O. K.; Roberts, J.; Scheidt, K. A.; Nguyen, S. T.; Hupp, J. T. *Chem. Soc. Rev.* **2009**, *38*, 1450. (b) Ma, L.; Abney, C.; Lin, W. *Chem. Soc. Rev.* **2009**, *38*, 1248. (c) Alkordi, M. H.; Liu, Y.; Larsen, R. W.; Eubank, J. F.; Eddaoudi, M. *J. Am. Chem. Soc.* **2008**, *130*, 12639.

(6) (a) Takashima, Y.; Martinez, V. M.; Furukawa, S.; Kondo, M.; Shimomura, S.; Uehara, H.; Nakahama, M.; Sugimoto, K.; Kitagawa, S. *Nat. Commun.* **2011**, *2*, 168. (b) Meilikhov, M.; Furukawa, S.; Hirai, K.; Fischer, R. A.; Kitagawa, S. *Angew. Chem., Int. Ed.* **2013**, *52*, 341. (c) Guo, Y.; Feng, X.; Han, T.; Wang, S.; Lin, Z.; Dong, Y.; Wang, B. *J. Am. Chem. Soc.* **2014**, *136*, 15485. (d) Li, H.; Feng, X.; Guo, Y.; Chen, D.; Li, R.; Ren, X.; Jiang, X.; Dong, Y.; Wang, B. *Sci. Rep.* **2014**, *4*, 4366.

(7) (a) Horcajada, P.; Chalati, T.; Serre, C.; Gillet, B.; Sebrie, C.; Baati, T.; Eubank, J. F.; Heurtaux, D.; Clayette, P.; Kreuz, C.; Chang, J.-S.; Hwang, Y. K.; Marsaud, V.; Bories, P.-N.; Cynober, L.; Gil, S.; Ferey, G.; Couvreur, P.; Gref, R. *Nat. Mater.* **2010**, *9*, 172. (b) Horcajada, P.; Serre, C.; Vallet-Regi, M.; Sebban, M.; Taulelle, F.; Ferey, G. *Angew. Chem., Int. Ed.* **2006**, *45*, 5974. (c) Kundu, T.; Mitra, S.; Patra, P.; Goswami, A.; Diaz Diaz, D.; Banerjee, R. *Chem.—Eur. J.* **2014**, *20*, 10514.

(8) (a) Allendorf, M. D.; Schwartzberg, A.; Stavila, V.; Talin, A. A. *Chem.—Eur. J.* **2011**, *17*, 11372. (b) Morozan, A.; Jaouen, F. *Energy Environ. Sci.* **2012**, *5*, 9269. (c) Han, Y.; Qi, P.; Li, S.; Feng, X.; Zhou, J.; Li, H.; Su, S.; Li, X.; Wang, B. *Chem. Commun.* **2014**, *50*, 8057.

(9) (a) Miles, D. O.; Jiang, D.; Burrows, A. D.; Halls, J. E.; Marken, F. *Electrochem. Commun.* **2013**, *27*, 9. (b) Yang, J.; Xiong, P.; Zheng, C.; Qiu, H.; Wei, M. *J. Mater. Chem. A* **2014**, *2*, 16640. (c) Díaz, R.; Orcajo, M. G.; Botas, J. A.; Calleja, G.; Palma, J. *Mater. Lett.* **2012**, *68*, 126. (d) Lee, D. Y.; Yoon, S. J.; Shrestha, N. K.; Lee, S.-H.; Ahn, H.; Han, S.-H. *Microporous Mesoporous Mater.* **2012**, *153*, 163.

(10) (a) Meng, F.; Fang, Z.; Li, Z.; Xu, W.; Wang, M.; Liu, Y.; Zhang, J.; Wang, W.; Zhao, D.; Guo, X. *J. Mater. Chem. A* **2013**, *1*, 7235. (b) Maiti, S.; Pramanik, A.; Mahanty, S. *Chem. Commun.* **2014**, *50*, 11717. (c) Zhang, Y.-Z.; Wang, Y.; Xie, Y.-L.; Cheng, T.; Lai, W.-Y.; Pang, H.; Huang, W. *Nanoscale* **2014**, *6*, 14354.

(11) (a) Liu, B.; Shioyama, H.; Akita, T.; Xu, Q. *J. Am. Chem. Soc.* **2008**, *130*, 5390. (b) Amali, A. J.; Sun, J.-K.; Xu, Q. *Chem. Commun.* **2014**, *50*, 1519. (c) Zhang, P.; Sun, F.; Shen, Z.; Cao, D. *J. Mater. Chem. A* **2014**, *2*, 12873. (d) Pachfule, P.; Biswal, B. P.; Banerjee, R. *Chem.—Eur. J.* **2012**, *18*, 11399.

(12) Choi, K. M.; Jeong, H. M.; Park, J. H.; Zhang, Y.-B.; Kang, J. K.; Yaghi, O. M. *ACS Nano* **2014**, *8*, 7451.

(13) (a) Zhang, T.; Lin, W. *Chem. Soc. Rev.* **2014**, *43*, 5982. (b) Wang, C.; Wang, J.-L.; Lin, W. *J. Am. Chem. Soc.* **2012**, *134*, 19895.

(14) (a) Chen, W.-C.; Wen, T.-C.; Teng, H. *Electrochim. Acta* **2003**, *48*, 641. (b) Lee, Y.; Chang, C.; Yau, S.; Fan, L.; Yang, Y.; Ou Yang, L.; Itaya, K. *J. Am. Chem. Soc.* **2009**, 6468.

(15) (a) Hu, C.-C.; Lin, J.-Y. *Electrochim. Acta* **2002**, *47*, 4055. (b) Zhang, L. L.; Li, S.; Zhang, J.; Guo, P.; Zheng, J.; Zhao, X. S. *Chem. Mater.* **2010**, *22*, 1195.

(16) Choi, B. G.; Hong, J.; Hong, W. H.; Hammond, P. T.; Park, H. *ACS Nano* **2011**, *5*, 7205.

(17) (a) Weng, Z.; Su, Y.; Wang, D.-W.; Li, F.; Du, J.; Cheng, H.-M. *Adv. Energy Mater.* **2011**, *1*, 917. (b) Xu, Y.; Lin, Z.; Huang, X.; Liu, Y.; Huang, Y.; Duan, X. *ACS Nano* **2013**, *7*, 4042. (c) Dong, X.; Wang, L.; Wang, D.; Li, C.; Jin, J. *Langmuir* **2012**, *28*, 293. (d) Xiao, X.; Peng, X.; Jin, H.; Li, T.; Zhang, C.; Gao, B.; Hu, B.; Huo, K.; Zhou, J. *Adv. Mater.* **2013**, *25*, 5091.

DOI: 10.1021/jacs.5b01613
J. Am. Chem. Soc. 2015, 137, 4920−4923